

UDC 548.73:541.49:542.72

**PROTONATED DIAMINES AS LINKERS IN THE SUPRAMOLECULAR ASSEMBLIES  
BASED ON THE  $[V_{12}B_{18}O_{60}H_6]$  POLYOXOVANADOBORATE ANION**

**P. Hermosilla-Ibáñez<sup>1,2</sup>, J. Costamagna<sup>1</sup>, A. Vega<sup>2,3</sup>, V. Paredes-García<sup>2,3</sup>, M.T. Garland<sup>4</sup>,  
E. Le Fur<sup>5,6</sup>, E. Spodine<sup>2,7</sup>, D. Venegas-Yazigi<sup>1,2</sup>**

<sup>1</sup>*Facultad de Química y Biología, Universidad de Santiago de Chile, Chile, USACH  
E-mail: diego.venegas@usach.cl*

<sup>2</sup>*CEDENNA, Chile*

<sup>3</sup>*Universidad Andres Bello, Departamento de Ciencias Químicas, Facultad de Ciencias Exactas, Chile*

<sup>4</sup>*Facultad de Ciencias Físicas y Matemáticas, Universidad de Chile, Chile*

<sup>5</sup>*ENSCR, CNRS, UMR 6226, Rennes, France*

<sup>6</sup>*Université Européenne de Bretagne, France*

<sup>7</sup>*Facultad de Ciencias Químicas y Farmacéuticas, Universidad de Chile, Chile*

Received February, 18, 2014

Two new polyoxovanadoborates based crystalline lattices are being reported:  $K_5(H_3O)_2(1,3\text{-diapH}_2)_2[V_{12}B_{18}O_{60}H_6] \cdot 10.80H_2O$  (**1**), and  $K_2(H_3O)_7(enH_2)[V_{12}B_{18}O_{60}H_6] \cdot 9H_2O$  (**2**). These structures are characterized by presenting multiple hydrogen bonds between the diprotonated diamines ( $enH_2$  and  $1,3\text{-diapH}_2$ ) and hydronium ions, and the oxygen atoms of the  $[V_{12}B_{18}O_{60}H_6]$  cluster. The crystalline packing and stability of these new polyoxovanadoborates is dominated by the different types of hydrogen interactions present in the lattices ranging from unidirectional to trifurcated ones. The crystallographic data, together with the BVS method, permit to assign a mixed valence ratios for the  $[V_{12}B_{18}O_{60}H_6]$  anionic cluster for (**1**) and (**2**) being 11/1 ( $V^{IV}/V^V$ ) ratio.

**Key words:** polyoxometalate, polyoxovanadate, supramolecular, mixed valence, BVO.

## INTRODUCTION

Organic amines as structural templates have been used to obtain new crystalline compounds with specific structural features such as porosity; these organic ligands serve in some cases to increase the dimensionality of the lattice [ 1—6 ].

Ethylenediamine, and 1,3-diaminopropane are among the most common used amines in reported polyoxometalate (POM) crystal lattices. Diamines can be found in the lattices acting as charge compensating agents, which implies that they are present as mono ( $diamineH^+$ ) or diprotonated ( $diamineH_2^{2+}$ ) species; they also can be present forming complexes. Thus, these complexes can be coordinated to the polyanions through the oxygen atoms or simply present in the crystalline lattice as charge compensating cationic complexes. Besides, protonated amines can stabilize the structure by hydrogen bond or electrostatic interactions. Moreover the dimensionality of the system can be increased when these cationic species act as bridges between the polyanionic units.

Some of the most known POMs correspond to the polyoxotungstates and polyoxomolybdates. As an illustrative example of the several roles that a diamine can present in a polyoxometallate crystalline lattice is  $[Cu(en)_2(OH_2)]_2[enH_2][\{Cu(en)_2\}P_2CuW_{17}O_{61}] \cdot 5H_2O$  [ 7 ]. In this structure ethylenediamine is present as ( $enH_2$ ) $^{2+}$  and  $[Cu(en)_2(OH_2)]^{2+}$  cationic species, which are not coordinated to the cluster,

and  $\{\text{Cu}(\text{en})_2\}^{2+}$  which is bonded to the POM through an oxygen atom of the polyoxophosphotungstate, forming a Cu—O bond. Another example is  $[\text{Cu}(\text{en})_2(\text{H}_2\text{O})]_2[\{\text{Cu}(\text{en})_2\}\text{H}_2\text{W}_{12}\text{O}_{40}] \cdot 10\text{H}_2\text{O}$  [8], in which ethylenediamine is present as a ligand coordinated to the  $\text{Cu}^{\text{II}}$  ions; the cationic complex  $\{\text{Cu}(\text{en})_2\}^{2+}$  is covalently bridging different polyanions through the oxygen atoms, thus increasing the dimensionality of the system. Besides, cationic  $[\text{Cu}(\text{en})_2(\text{H}_2\text{O})]^{2+}$  complexes are present in this crystalline lattice as charge compensating ions.

A recently investigated family of POMs is the polyoxovanadoborate (BVO) [9], which presents different stoichiometric vanadium/boron ratios and different mixed valence  $\text{V}^{\text{IV}}/\text{V}^{\text{V}}$  ratios. The following compounds have been reported in the literature with different V/B ratios and in which ethylenediamine and 1,3-diaminopropane, with different degree of protonation, are present in the crystalline lattice:  $[\text{V}_6\text{B}_{20}]$ ,  $[\text{enH}_2]_4[\text{enH}]_2[\text{B}_2\text{O}_3\text{H}_2][\text{V}_6\text{B}_{20}\text{O}_{50}\text{H}_6] \cdot 5\text{H}_2\text{O}$  [10],  $(\text{enH}_2)_4[(\text{VO})_6(\text{B}_{10}\text{O}_{22})_2] \cdot (\text{H}_3\text{O})_7$  [11],  $(\text{enH})_3\{\text{VO}\}_6[\text{B}_{10}\text{O}_{16}(\text{OH})_6]_2 \cdot 11\text{H}_2\text{O}$  [12],  $[\text{V}_{10}\text{B}_{28}]$ ,  $\text{Na}_2(\text{H}_2\text{en})_2 \cdot n(\text{H}_2\text{O})_2 \cdot (\text{H}_3\text{O})_{12}\{\text{VO}\}_{10} \cdot [\text{B}_{14}\text{O}_{30}(\text{OH})_2]_2\{\text{Mn}_4(\text{C}_2\text{O}_4)[\text{B}_2\text{O}_4(\text{OH})_2]_2\}(\text{H}_2\text{O})_{19}$ , [13];  $[\text{V}_{12}\text{B}_{16}]$ ,  $(\text{enH}_2)_4[(\text{VO})_{12}\text{O}_4\{\text{B}_8\text{O}_{17}(\text{OH})_4\}_2 \cdot \{\text{Mn}(\text{H}_2\text{O})_2\}_2] \cdot \text{H}_2\text{O}$  [14],  $(\text{enH}_2)_3(\text{H}_3\text{O})_2[(\text{VO})_{12}\text{O}_4\{\text{B}_8\text{O}_{17}(\text{OH})_4\}_2\{\text{Na}(\text{H}_2\text{O})\}_2] \cdot 6.5(\text{H}_2\text{O})$  [15],  $\text{Na}[\text{V}_{12}\text{B}_{16}\text{O}_{50}(\text{OH})_7(\text{en})]_2(\text{enH}_2)_6(\text{enH})_2(\text{OH})(\text{H}_2\text{O})_{19}$  [16],  $[\text{V}_{12}\text{B}_{17}]$ ,  $(\text{enH})(\text{enH}_2)_4[(\text{VO})_{12}\text{B}_{17}\text{O}_{38} \cdot (\text{OH})_8] \cdot \text{H}_2\text{O}$  [17],  $[\text{V}_{12}\text{B}_{18}]$ ,  $(1,3\text{-diapH}_2)_5[\text{V}_{12}\text{B}_{18}\text{O}_{60}\text{H}_6] \cdot 6\text{H}_2\text{O}$  [17],  $(\text{enH}_2)_4\text{Na}_4\text{H}_3 \cdot [\text{VO}]_{12}\text{O}_6\text{B}_{18}\text{O}_{42}] \cdot 8\text{H}_2\text{O}$  [18],  $\text{K}_3\text{Na}_5(\text{enH}_2)_2\{(\text{VO})_{12}\text{O}_6[\text{B}_3\text{O}_6(\text{OH})]_6\}(\text{H}_2\text{O}) \cdot 12\text{H}_2\text{O}$  [19].

To the best of our knowledge for all the BVO family only one crystalline lattice with 1,3-diaminopropane has been reported (CCDC code REGHEQ) [17].

In all the above mentioned clusters the vanadium atoms present square base pyramidal geometry, while the boron atoms present both trigonal and tetrahedral geometries. The above mentioned BVO clusters stabilize their negative charge with metal and hydronium ions and amines with different degrees of protonation. These charge compensating species are acting as connectors, increasing the dimensionality of the system from 0D to 1D, 2D or 3D.

In the present work, the synthesis and structural characterization of two new polyoxovanadoborates (BVO) based on the  $[\text{V}_{12}\text{B}_{18}\text{O}_{60}\text{H}_6]^{n-}$  polyanion are reported.

The negative charge is neutralized by diprotonated diamines ( $1,3\text{-diapH}_2 = 1,3$  propanediammonium and  $\text{enH}_2 = \text{ethylenediammonium}$ ) and secondary cations such as potassium, and hydronium:  $\text{K}_5(\text{H}_3\text{O})_2(1,3\text{-diapH}_2)_2[\text{V}_{12}\text{B}_{18}\text{O}_{60}\text{H}_6] \cdot 10.8\text{H}_2\text{O}$  (**1**),  $\text{K}_2(\text{H}_3\text{O})_7(\text{enH}_2)[\text{V}_{12}\text{B}_{18}\text{O}_{60}\text{H}_6] \cdot 9.0\text{H}_2\text{O}$  (**2**).

## EXPERIMENTAL

**K<sub>5</sub>(H<sub>3</sub>O)<sub>2</sub>(1,3-diapH<sub>2</sub>)<sub>2</sub>[V<sub>12</sub>B<sub>18</sub>O<sub>60</sub>H<sub>6</sub>] · 10.8H<sub>2</sub>O (1).** A mixture of  $\text{V}_2\text{O}_5$  (0.1818 g, 1.00 mmol),  $\text{H}_3\text{BO}_3$  (1.0000 g, 16.0 mmol),  $\text{K}_2\text{HPO}_4$  (0.2612 g, 1.50 mmol),  $\text{MnCl}_2 \cdot 4\text{H}_2\text{O}$  (0.3237 g, 2.00 mmol),  $\text{H}_2\text{O}$  (2.0 mL, 111 mmol) and 1,3-diaminopropane (0.4 mL, 6.00 mmol) was transferred into a 23 mL teflon lined Parr reactor and heated at 180 °C for 5 days. The initial pH value of the reacting mixture was 10.35 and the final pH value was 10.06. After cooling the reaction mixture to room temperature dark red crystals, together with other solid phases, were collected by filtration and mechanically separated under a microscope. The crystals were washed with water and dried at room temperature. Yield: (0.1400 g, 36 % based on V). Even though  $\text{Mn}^{\text{II}}$  ions are not present in the final crystalline packing, this lattice is not formed in the absence of the  $\text{Mn}^{\text{II}}$  salt.

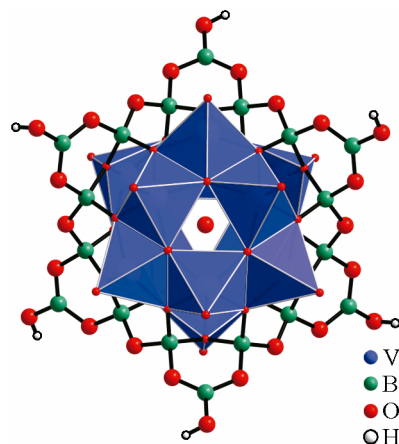
**K<sub>2</sub>(H<sub>3</sub>O)<sub>7</sub>(enH<sub>2</sub>)[V<sub>12</sub>B<sub>18</sub>O<sub>60</sub>H<sub>6</sub>] · 9.0H<sub>2</sub>O (2).** A mixture of  $\text{V}_2\text{O}_5$  (0.1818 g, 1.00 mmol),  $\text{H}_3\text{BO}_3$  (1.0000 g, 16.0 mmol),  $\text{K}_2\text{HPO}_4$  (0.2612 g, 1.50 mmol),  $\text{MnCl}_2 \cdot 4\text{H}_2\text{O}$  (0.3237 g, 2.00 mmol),  $\text{H}_2\text{O}$  (2.0 mL, 111 mmol) and ethylenediamine (0.4 mL, 6.00 mmol) was transferred into a 23 mL teflon lined Parr reactor and heated at 180 °C for 5 days. The initial pH value of the reacting mixture was 10.01 and the final pH value was 9.80. After cooling the reaction mixture to room temperature dark red crystals, together with other solid phases, were collected by filtration and mechanically separated under a microscope. The crystals were washed with water and dried at room temperature. Yield: (0.1270 g, 35 % based on V). Compound (**4**) is only formed when the  $\text{Mn}^{\text{II}}$  salt is added.

**Crystal structure determination.** A single crystal for each compound was taken directly from the synthesis vessel and examined under microscope, suggesting acceptable quality. It was then mounted on the tip of a glass fiber. Preliminary examination with X-ray confirms the quality suggested

by microscopy, proceeding to full data collection. The intensities for (**1**) and (**2**) were recorded at room temperature on a Bruker Smart Apex diffractometer, using separations of  $0.3^\circ$  between frames and 10s by frame. Data integration was made using SAINTPLUS [20]. The structures were solved by direct methods using XS in SHELXTL [21] and completed (non-H atoms) by Fourier difference synthesis. Refinement until convergence was obtained using XL SHELXTL [22] and SHELXL97 [23]. The H-atom positions were calculated after each cycle of refinement using a riding model, with C—H =  $0.97\text{ \AA}$  and  $U_{\text{iso}}(\text{H}) = 1.2U_{\text{eq}}(\text{parent})$  and N—H =  $0.89$  or  $0.91\text{ \AA}$  and  $U_{\text{iso}}(\text{H}) = 1.5U_{\text{eq}}(\text{parent})$ . Efforts to locate the borovanadate H atoms in the final Fourier difference map were unsuccessful; those reported for the formula are based on literature data. For (**1**) the occupancy of potassium atoms K3 and K4 was refined, and finally set equal to 0.40 and 0.60 respectively. The 12.80 oxygen atoms corresponding to solvating intermolecular water molecules and/or hydronium ions were modelled using partial occupancies (refined and then held constant) over 24 different positions: O32w, O33w, O34w, O35w and O40w (0.40); O36w and O39w (0.2); O37w (0.3); O38w (0.6) and O41w (0.8). Disorder on the 1,3-diap was modelled using two different positions, A and B, for atoms C1 and N1. The occupancies were refined and then held constant at 0.75/0.25 for A and B respectively. For (**2**) 16 water molecules and/or hydronium oxygen atoms are spread over 54 positions. The partial occupancies for oxygen atoms were O66w, O67w, O69w, O70w, O71w, O72w, O74w, O76w, O77w, O78w, O79w, O80w and O81w (0.5); O68w and O73w (0.75); O82w, O83w, O84w, O85w and O86w (0.25). Efforts for lowering the rather high residuals on the refinement for each compound included the evaluation of different models of solvation, and the use of squeeze for the modelling of the remaining electronic density was unsuccessful. Some parameters remained high; this should be considered as arising from the complexity of the model used for the solvation and counterbalancing. Moreover, it is not related to the main characteristics of the structures, whose determination should still be considered as correct. Additional details on data collection are listed in Table 1. Structure drawings were carried out with DIAMOND-3.2i, supplied by Crystal Impact [24].

T a b l e 1  
Crystal data and structure refinement for complexes **1** and **2**

Complex	<b>1</b>	<b>2</b>
Formula	$\text{C}_6\text{H}_{56.6}\text{B}_{18}\text{K}_5\text{N}_4\text{O}_{72.80}\text{V}_{12}$	$\text{C}_2\text{H}_{55}\text{B}_{18}\text{K}_2\text{N}_2\text{O}_{76}\text{V}_{12}$
Moietiy formula	$\text{K}_5(\text{H}_3\text{O})_2(1,3\text{-diapH}_2)[\text{V}_{12}\text{B}_{18}\text{O}_{60}\text{H}_6] \cdot 10.8\text{H}_2\text{O}$	$\text{K}_2(\text{H}_3\text{O})_7(\text{enH}_2)[\text{V}_{12}\text{B}_{18}\text{O}_{60}\text{H}_6] \cdot 9.0\text{H}_2\text{O}$
Formula weight	2352.44	2207.65
Temperature, K	150(2)	297(2)
Crystal system	Monoclinic	Triclinic
Space group	$C2/c$	$P\bar{1}$
$a, b, c, \text{\AA}$	22.387(2), 15.4548(15), 21.701(2)	13.587(2), 13.698(2), 21.743(4)
$\alpha, \beta, \gamma, \text{deg.}$	90.00, 107.703(2), 90.00	75.185(3), 75.616(3), 67.959(3)
Volume, $\text{\AA}^3$	7152.5(12)	3573.2(11)
$Z$	4	2
Density (calculated), $\text{g/cm}^3$	2.153	2.010
Absorption coefficient, $\text{mm}^{-1}$	1.918	1.744
$F(000)$	4525.6	2096.0
Crystal size, mm	$0.38 \times 0.16 \times 0.14$	$0.29 \times 0.13 \times 0.07$
$\theta$ range for data collection, deg.	1.63 to 25.03	1.85 to 25.08
Index ranges	$-25 \leq h \leq 26, -18 \leq k \leq 18,$ $-25 \leq l \leq 25$	$-16 \leq h \leq 16, -16 \leq k \leq 16,$ $-25 \leq l \leq 25$
Reflections collected	21890	22041
Independent reflections	6319 [ $R(\text{int}) = 0.0245$ ]	12690 [ $R(\text{int}) = 0.0564$ ]
Refinement method	Full-matrix least-squares on $F^2$	Full-matrix least-squares on $F^2$
Goodness-of-fit on $F^2$	1.089	1.060
Final $R$ indices [ $I > 2\sigma(I)$ ]	$R_1 = 0.0536, wR_2 = 0.1627$	$R_1 = 0.1021, wR_2 = 0.2784$
$R$ indices (all data)	$R_1 = 0.0581, wR_2 = 0.1676$	$R_1 = 0.1271, wR_2 = 0.3002$
Largest diff. peak and hole, $e/\text{\AA}^{-3}$	1.78 and -1.53	1.97 and -2.13

Fig. 1. Scheme showing the  $[V_{12}B_{18}O_{60}H_6]$  anionic cluster

**Description of crystal structures.** Compound (1) crystallizes in the monoclinic system with space group  $C2/c$ , while (2) presents a lower symmetry with a triclinic system in a space group  $P\bar{1}$ . The symmetry group of the polyanion is  $C_i$  in both cases.

The crystalline lattice of (1) and (2) is based on the  $[V_{12}B_{18}O_{60}H_6]^{n-}$  polyanion. This polyanion is formed by the condensation of two hexanuclear units of oxovanadate  $[V_6O_9]^{n+}$  with a  $[B_{18}O_{36}(OH)_6]^{24-}$  borate ring. This ring is located in the centre of the cluster, containing an occluded water molecule (Fig. 1). All the vanadium atoms present a square base pyramidal geometry, while the boron atoms adopt both, trigonal (trig) and tetrahedral (tet) geometries, as reported before for this type of clusters. For the crystallographic description of the supramolecular assemblies, distances up to 3.1 Å were considered to define hydrogen bond and alkaline ion-oxygen atom interactions [25–28].

**K<sub>5</sub>(H<sub>3</sub>O)<sub>2</sub>(1,3-diapH<sub>2</sub>)<sub>2</sub>[V<sub>12</sub>B<sub>18</sub>O<sub>60</sub>H<sub>6</sub>]·10.8H<sub>2</sub>O (1).** Selected V—O and B—O distances and O—V—O and O—B—O bond angles for (1) are given in Table 2. The crystalline lattice of (1) presents 1,3-propilendiamonium (1,3-diapH<sub>2</sub>), potassium and hydronium cations, which counterbalance the negative charge of the  $[V_{12}B_{18}O_{60}H_6]$  polyanion. These cations produce a stabilizing effect of the crystalline lattice.

Fig. 2, A shows the hydrogen bonds present in the crystalline structure, specifically those which permit the connection of the polyanions through the 1,3-propilendiamonium. Each 1,3-diapH<sub>2</sub> links three anionic clusters (Fig. 2, B) through the following hydrogen bonds: N1A—H1AC···O15, N1A—H1AD···O22<sup>vii</sup>, N2—H2C···O41W<sup>viii</sup>, N2—H2D···O10<sup>iii</sup>, N2—H2E···O25<sup>vii</sup>, N2—H2E···O25<sup>ix</sup>, being the (N2—H2E) a bifurcated hydrogen bond; the corresponding bond distances are: 2.889(7) Å, 2.790(7) Å, 2.911(9) Å, 2.955(6) Å, 2.960(6) and 2.981(5) Å, respectively (Fig. 2, A and Table 3). Fig. 3 shows the crystalline lattice and the spatial orientation of the protonated diamines, which are all oriented in the same direction, but not along a specific crystallographic axis.

This crystalline lattice presents besides the diprotonated diamine, four potassium ions with different crystallographic sites, K1, K2, K3 and K4. These potassium ions have different coordination environments, being hepta-coordinated (K1, K4), octa-coordinated (K2) and hexa-coordinated (K3).

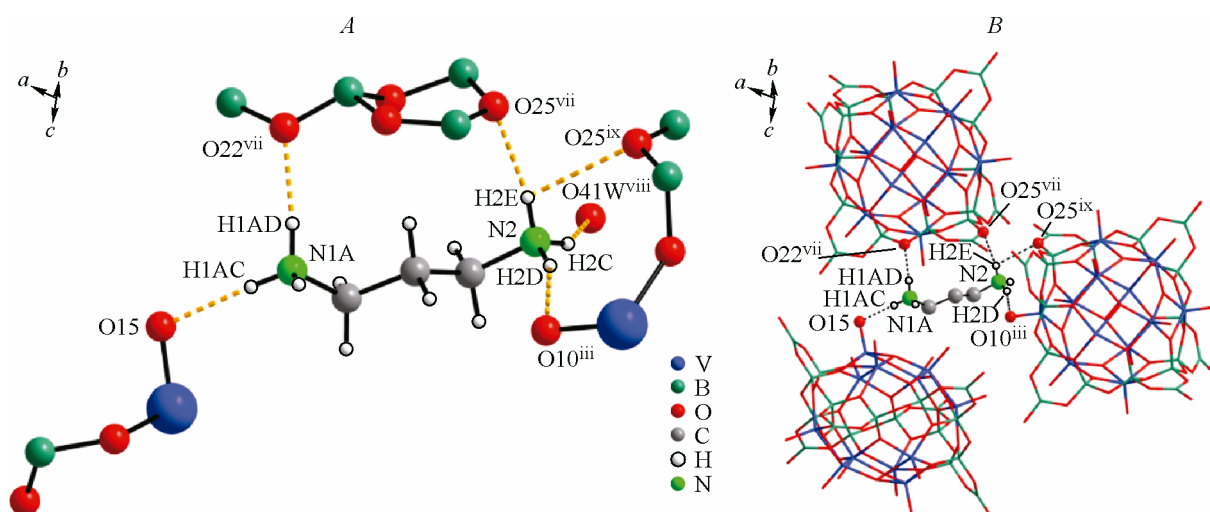
Fig. 2. Detail of the different modes of hydrogen bonding in 1 (A). Scheme showing the connectivity of the 1,3-diapH<sub>2</sub> cation with three BVO clusters for 1 (B)

Table 2

Selected bond distances ( $\text{\AA}$ ) and angles (deg.) for compound 1

V1—O10	1.622(3)	V5—O7	1.934(3)	B4—O9 <sup>i</sup>	1.476(7)
V1—O2	1.933(3)	V5—O9	1.936(3)	B4—O23	1.482(6)
V1—O3	1.942(4)	V5—O8	1.962(3)	B4—O14	1.509(7)
V1—O1	1.950(3)	V5—O17	2.011(3)	B5—O25	1.353(7)
V1—O11	1.991(3)	V6—O18	1.622(4)	B5—O23	1.362(7)
V2—O12	1.618(4)	V6—O1	1.908(3)	B5—O24	1.369(7)
V2—O1	1.917(3)	V6—O8	1.916(3)	B6—O26	1.431(7)
V2—O4	1.918(3)	V6—O9	1.944(3)	B6—O2 <sup>i</sup>	1.475(6)
V2—O5	1.945(3)	V6—O2	1.952(3)	B6—O25	1.474(6)
V2—O3	1.958(4)	B1—O30 <sup>i</sup>	1.435(7)	B6—O14	1.521(6)
V3—O13	1.623(4)	B1—O3	1.468(6)	B7—O26	1.431(6)
V3—O6	1.932(3)	B1—O19	1.491(6)	B7—O6	1.477(6)
V3—O5	1.938(3)	B1—O17 <sup>i</sup>	1.517(6)	B7—O27	1.481(6)
V3—O4	1.954(3)	B2—O21	1.358(7)	B7—O11 <sup>i</sup>	1.523(6)
V3—O14	2.017(3)	B2—O20	1.366(7)	B8—O27	1.351(7)
V4—O15	1.626(4)	B2—O19	1.379(7)	B8—O29	1.356(7)
V4—O4	1.923(3)	B3—O22	1.439(6)	B8—O28	1.386(7)
V4—O8	1.925(3)	B3—O21	1.465(6)	B9—O30	1.442(7)
V4—O6	1.942(3)	B3—O5	1.477(6)	B9—O29	1.468(6)
V4—O7	1.951(3)	B3—O17 <sup>i</sup>	1.518(6)	B9—O7	1.478(6)
V5—O16	1.616(4)	B4—O22	1.438(6)	B9—O11 <sup>i</sup>	1.517(6)
O10—V1—O2	108.40(16)	O8—V4—O6	145.30(15)	O4—V4—O7	146.11(15)
O10—V1—O3	108.02(17)	O15—V4—O7	107.53(17)	O8—V4—O7	79.58(14)
O2—V1—O3	141.02(15)	O5—B3—O17 <sup>i</sup>	108.2(4)	O6—V4—O7	88.00(14)
O10—V1—O1	107.38(17)	O22—B4—O9 <sup>i</sup>	110.4(4)	O16—V5—O7	108.70(18)
O2—V1—O1	78.04(14)	O22—B4—O23	107.2(4)	O16—V5—O9	111.72(18)
O3—V1—O1	78.31(14)	O9 <sup>i</sup> —B4—O23	109.0(4)	O7—V5—O9	137.52(15)
O10—V1—O11	107.52(16)	O22—B4—O14	112.4(4)	O16—V5—O8	107.17(18)
O2—V1—O11	91.41(14)	O9 <sup>i</sup> —B4—O14	107.7(4)	O7—V5—O8	79.07(14)
O3—V1—O11	90.58(14)	O23—B4—O14	110.0(4)	O9—V5—O8	77.14(14)
O1—V1—O11	145.10(14)	O25—B5—O23	122.1(5)	O16—V5—O17	106.41(17)
O12—V2—O1	108.36(17)	O25—B5—O24	120.4(5)	O7—V5—O17	91.22(14)
O12—V2—O4	109.31(18)	O23—B5—O24	117.5(5)	O9—V5—O17	89.59(14)
O1—V2—O4	91.59(15)	O26—B6—O2 <sup>i</sup>	110.3(4)	O8—V5—O17	146.40(15)
O12—V2—O5	109.37(18)	O26—B6—O25	107.5(4)	O18—V6—O1	108.95(17)
O1—V2—O5	142.15(15)	O2 <sup>i</sup> —B6—O25	109.8(4)	O18—V6—O8	107.85(18)
O4—V2—O5	78.80(14)	O26—B6—O14	113.5(4)	O1—V6—O8	92.83(15)
O12—V2—O3	105.39(18)	O2 <sup>i</sup> —B6—O14	108.0(4)	O18—V6—O9	110.50(18)
O1—V2—O3	78.71(14)	O25—B6—O14	107.7(4)	O1—V6—O9	140.44(15)
O4—V2—O3	145.27(15)	O26—B7—O6	110.6(4)	O8—V6—O9	78.04(14)
O5—V2—O3	88.61(15)	O26—B7—O27	107.1(4)	O8—V6—O2	145.17(15)
O13—V3—O6	108.02(17)	O6—B7—O27	109.8(4)	O9—V6—O2	87.32(14)
O13—V3—O5	112.11(17)	O26—B7—O11 <sup>i</sup>	112.9(4)	O30 <sup>i</sup> —B1—O3	111.2(4)
O6—V3—O5	137.87(16)	O6—B7—O11 <sup>i</sup>	107.2(4)	O30 <sup>i</sup> —B1—O19	108.0(4)
O13—V3—O4	106.87(17)	O27—B7—O11 <sup>i</sup>	109.3(4)	O3—B1—O19	108.4(4)
O6—V3—O4	78.58(14)	O27—B8—O29	122.3(5)	O30 <sup>i</sup> —B1—O17 <sup>i</sup>	112.3(4)

Continued Table 2

O5—V3—O4	78.07(14)	O27—B8—O28	117.8(5)	O3—B1—O17 <sup>i</sup>	108.4(4)
O13—V3—O14	107.76(17)	O29—B8—O28	119.9(5)	O19—B1—O17 <sup>i</sup>	108.4(4)
O6—V3—O14	90.53(14)	O30—B9—O29	107.5(4)	O21—B2—O20	118.4(5)
O5—V3—O14	89.20(14)	O30—B9—O7	110.0(4)	O21—B2—O19	121.4(5)
O4—V3—O14	145.37(14)	O29—B9—O7	109.8(4)	O20—B2—O19	120.2(5)
O15—V4—O4	106.25(17)	O30—B9—O11 <sup>i</sup>	113.9(4)	O22—B3—O21	106.9(4)
O15—V4—O8	106.48(17)	O29—B9—O11 <sup>i</sup>	108.0(4)	O22—B3—O5	110.2(4)
O4—V4—O8	93.42(15)	O7—B9—O11 <sup>i</sup>	107.5(4)	O21—B3—O5	110.1(4)
O15—V4—O6	108.15(17)	O18—V6—O2	106.86(17)	O22—B3—O17 <sup>i</sup>	112.0(4)
O4—V4—O6	79.09(14)	O1—V6—O2	78.58(14)	O21—B3—O17 <sup>i</sup>	109.4(4)

Symmetry codes: <sup>i</sup>  $-x+3/2, -y+1/2, -z+1$ .

Table 3

#### Hydrogen-bond geometry for compound 1

$D—H\cdots A$	$D—H$	$H\cdots A$	$D\cdots A$	$D—H\cdots A$
N1A—H1AC···O15	0.91	1.98	2.889(7)	174
N1A—H1AD···O22 <sup>vii</sup>	0.91	1.89	2.790(7)	172
N2—H2C···O41W <sup>viii</sup>	0.91	2.12	2.911(9)	145
N2—H2D···O10 <sup>iii</sup>	0.91	2.09	2.955(6)	159
N2—H2E···O25 <sup>vii</sup>	0.91	2.07	2.960(6)	166
N2—H2E···O25 <sup>ix</sup>	0.91	2.54	2.981(5)	110

Symmetry codes: <sup>iii</sup>  $1-x, y, 1/2-z$ ; <sup>vii</sup>  $3/2-x, 1/2+y, 1/2-z$ ;  
<sup>viii</sup>  $-1/2+x, 1/2+y, z$ ; <sup>ix</sup>  $-1/2+x, 1/2-y, -1/2+z$ .

The coordination environment of K1 is defined by three POM units and two water molecules, through the following interactions K1—O20—(BO<sub>2</sub>) (2.865 Å) POM1, K1—O29 (2.779 Å) and K1—O15—(V) (2.922 Å) POM2, K1—O29 (2.845 Å) and K1—O30 (3.009 Å) POM3, K1—O30w (2.650 Å) and K1—O31w (2.788 Å), (Fig. 4, a).

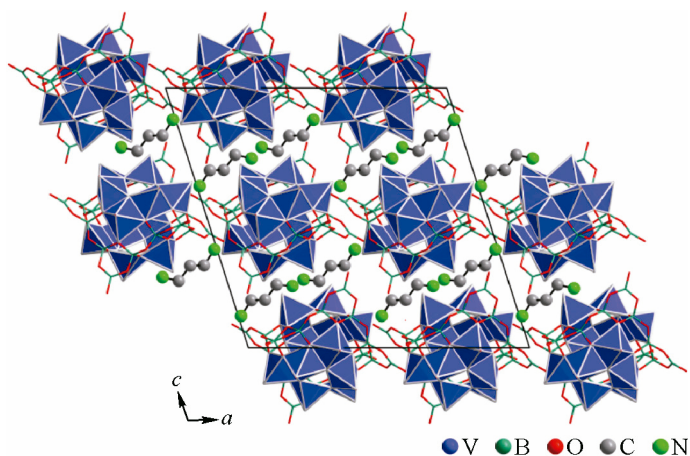


Fig. 3. View of the crystalline packing of 1 in the plane (0 1 0)

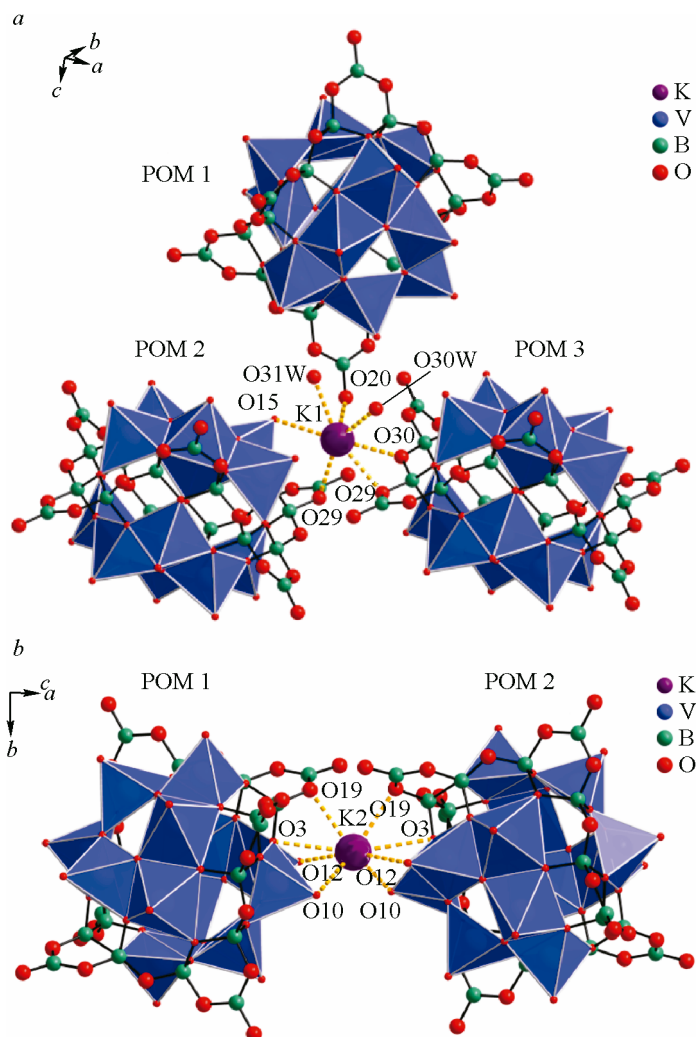


Fig. 4. Coordination spheres of K1 for **1** (a) and K2 for **1** (b)

The coordination number of K2 is eight, generated by the interaction of two POM units through K2—O3, K2—O10, K2—O12 and K2—O19 present for each cluster. The corresponding distances for the above mentioned bonds are 3.098 Å, 2.805 Å, 2.889 Å and 2.871 Å, respectively (Fig. 4, b).

The environment around K3 is slightly different, showing coordination to only one POM unit through two vanadyl oxygen atoms (K3—O16: 2.924; K3—O18: 2.839 Å). The other coordination sites are occupied by water molecules (K3—O31w: 2.641; K3—O32w: 2.666; K3—O33w: 2.963 Å; K3—O34w: 2.766 Å) (Fig. 5, a).

The last potassium ion, K4, is also connected to one POM unit; however, it presents two bonds to vanadyl oxygen atoms and one bond to an oxygen atom of a trigonal boron (K4—O13: 3.020; K4—O15: 2.735; K4—O27: 3.109 Å). The other four coordination sites correspond to oxygen atoms of water molecules (K4—O33w: 2.881; K4—O35w: 2.849; K4—O39w: 2.627; K4—O40w: 2.551 Å), thus making this potassium ion hepta-coordinated (Fig. 5, b).

**K<sub>2</sub>(H<sub>3</sub>O)<sub>7</sub>(enH<sub>2</sub>)**[V<sub>12</sub>B<sub>18</sub>O<sub>60</sub>H<sub>6</sub>]**·9.0H<sub>2</sub>O (2).**** Selected V—O and B—O distances and O—V—O and O—B—O bond angles for (2) are given in Table 4.**

The crystalline lattice of compound (2) is stabilized by hydrogen bond interactions between the diprotonated ethylenediamine with three clusters (Fig. 6, A). This diammmonium cation shows several hydrogen bonds: one trifurcated, two bifurcated and three simple bonds (Fig. 6, B). The trifurcated interaction occurs at the following atoms: N2—H2D···O43<sup>vi</sup>(2.910(2) Å), N2—H2D···O20<sup>vii</sup>

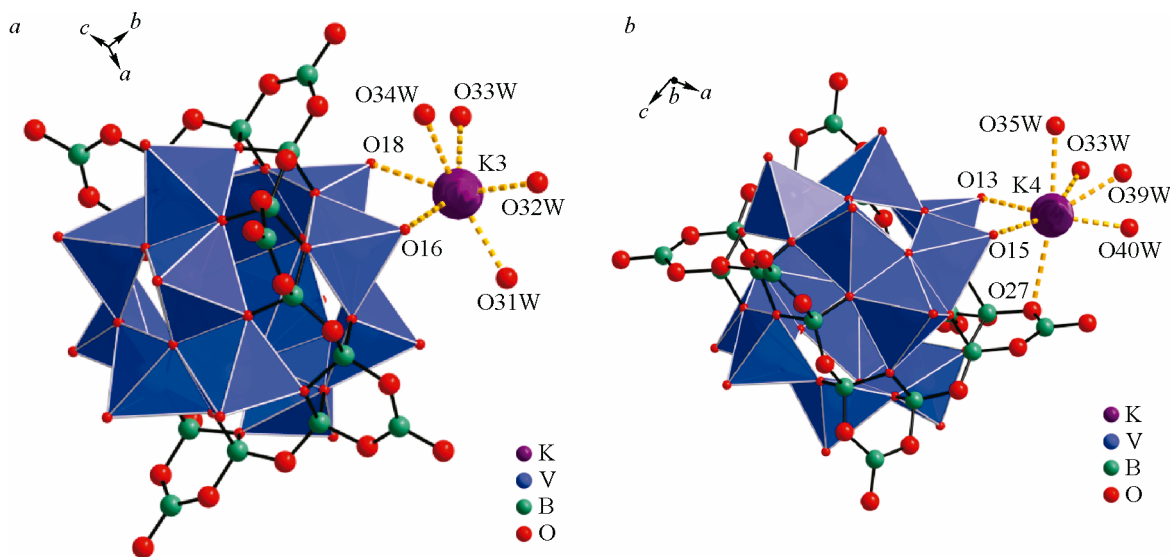


Fig. 5. Coordination spheres of K3 for **1** (*a*) and K4 for **1** (*b*)

(2.850(2) Å), N2—H2D···O69<sup>W</sup><sup>viii</sup> (2.980(2) Å) corresponding to POM2, POM3 and a water molecule respectively. One bifurcated bond to POM3, N2—H2E···O13<sup>iv</sup> (3.010(2) Å), N2—H2E···O20<sup>vii</sup> (2.850(2) Å), and the second bifurcated bond to POM2 and POM3, N1—H1D···O43<sup>vi</sup> (2.934(13) Å), N1—H1D···O21<sup>vii</sup> (2.930(14) Å). The three single bonds correspond to N1—H1C···O49<sup>v</sup> (2.823(13) Å), N1—H1E···O49<sup>vi</sup> (2.830(14) Å), N2—H2C···O12<sup>iv</sup> (2.930(2) Å) interacting to POM1, 2 and 3 respectively (Fig. 6, B and Table 5). This crystalline packing also presents an orderly distribution of the protonated diamine ions (Fig. 7).

In this structure two different crystallographic sites for the potassium cations, K1 and K2, can be described (Fig. 8). A hepta-coordinated environment can be defined for K1. This potassium ion is connected to POM1 through the following four interactions: K1—O59 ( $B_{\text{trig}}$ —O59— $B_{\text{tet}}$ ), 2.856 Å; K1—O39, 3.091 Å; K1—O40 (O vanadyl), 2.815 Å and K1—O60 (O vanadyl), 2.909 Å. The other three interactions are to POM2: K1—O13 (O vanadyl), 2.887 Å; K1—O14 (O vanadyl), 2.791 Å and K1—O19 ( $B_{\text{trig}}$ —O19— $B_{\text{tet}}$ ), 2.950 Å. K2 is hexa-coordinated and connects to two vicinal POM

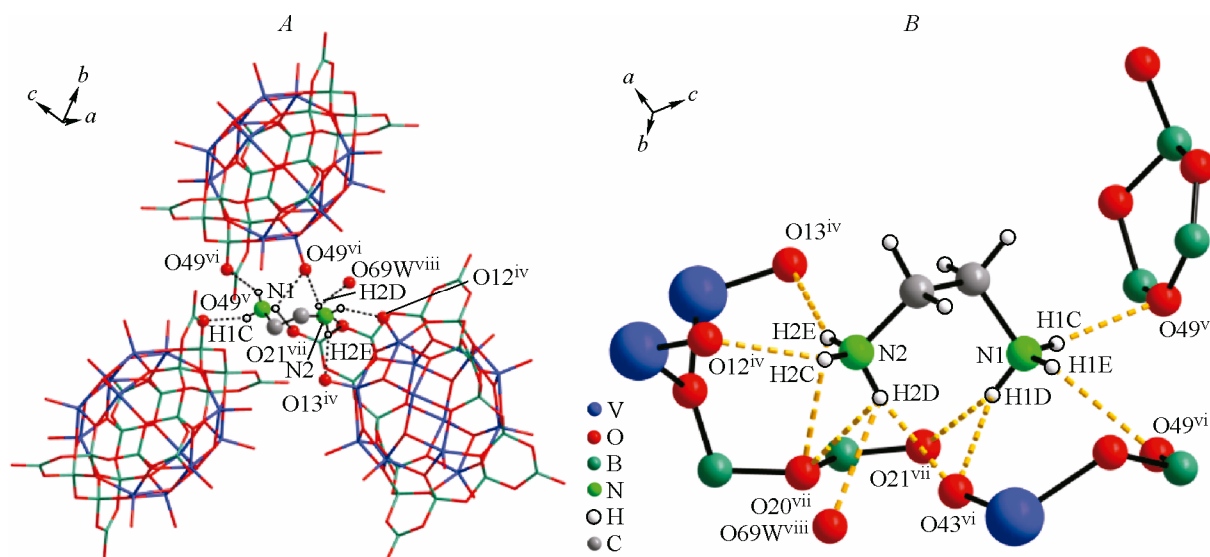


Fig. 6. Scheme showing the connectivity for **2** of the enH<sub>2</sub> cation with three BVO clusters (*A*). Detail of the different modes of hydrogen bonding for the enH<sub>2</sub> in **2** (*B*)

Table 4

Selected bond distances ( $\text{\AA}$ ) and angles (deg.) for compound 2

V1—O10	1.621(8)	V5—O9	1.929(7)	O18—B4	1.528(13)
V1—O1	1.951(7)	V5—O7	1.942(7)	O23—B4	1.490(14)
V1—O3	1.953(7)	V5—O8	1.951(7)	O3—B4 <sup>i</sup>	1.490(13)
V1—O2	1.958(7)	V5—O18	2.003(7)	O23—B5	1.359(14)
V1—O16	1.997(7)	V6—O15	1.623(8)	O24—B5	1.389(14)
V2—O11	1.639(8)	V6—O2	1.910(7)	O25—B5	1.350(14)
V2—O4	1.920(7)	V6—O8	1.937(7)	O5—B6 <sup>i</sup>	1.502(13)
V2—O2	1.941(7)	V6—O1	1.962(8)	O18—B6	1.514(14)
V2—O3	1.944(7)	V6—O9	1.962(7)	O25—B6	1.468(14)
V2—O5	1.955(7)	O19—B1	1.363(14)	O26—B6	1.448(14)
V3—O12	1.629(8)	O20—B1	1.364(14)	O9—B7	1.475(15)
V3—O5	1.930(7)	O21—B1	1.377(14)	O17—B7 <sup>i</sup>	1.521(13)
V3—O6	1.933(7)	O16—B2	1.506(13)	O26—B7	1.432(14)
V3—O4	1.955(7)	O19—B2	1.502(12)	O27—B7	1.508(14)
V3—O17	2.022(8)	O7—B2 <sup>i</sup>	1.473(14)	O27—B8	1.364(14)
V4—O13	1.640(7)	O22—B2 <sup>i</sup>	1.449(13)	O28—B8	1.354(15)
V4—O8	1.930(7)	O16—B3 <sup>i</sup>	1.511(14)	O29—B8	1.363(14)
V4—O4	1.933(7)	O20—B3 <sup>i</sup>	1.486(13)	O1—B9	1.439(15)
V4—O7	1.961(7)	O6—B3	1.459(15)	O17—B9 <sup>i</sup>	1.540(15)
V4—O6	1.968(7)	O30—B3 <sup>i</sup>	1.462(14)	O29—B9	1.477(14)
V5—O14	1.631(7)	O22—B4	1.428(13)	O30—B9	1.447(13)
O10—V1—O1	110.3(4)	O4—V4—O7	144.5(3)	O7—V4—O6	88.3(3)
O10—V1—O3	107.5(4)	O13—V4—O6	106.9(4)	O14—V5—O9	109.4(3)
O1—V1—O3	140.0(3)	O20 <sup>i</sup> —B3—O16 <sup>i</sup>	109.8(8)	O14—V5—O7	108.8(4)
O10—V1—O2	108.4(4)	O22—B4—O3 <sup>i</sup>	111.2(8)	O9—V5—O7	139.5(3)
O1—V1—O2	77.8(3)	O22—B4—O23	107.0(8)	O14—V5—O8	106.5(4)
O3—V1—O2	78.2(3)	O3 <sup>i</sup> —B4—O23	109.0(9)	O9—V5—O8	78.2(3)
O10—V1—O16	106.4(4)	O22—B4—O18	114.4(9)	O7—V5—O8	78.5(3)
O1—V1—O16	91.2(3)	O3 <sup>i</sup> —B4—O18	107.7(8)	O14—V5—O18	108.4(3)
O3—V1—O16	90.5(3)	O23—B4—O18	107.5(8)	O9—V5—O18	90.8(3)
O2—V1—O16	145.2(3)	O25—B5—O23	122.7(10)	O7—V5—O18	89.7(3)
O11—V2—O4	106.7(3)	O25—B5—O24	117.1(10)	O8—V5—O18	145.1(3)
O11—V2—O2	106.9(4)	O23—B5—O24	120.1(10)	O15—V6—O2	109.5(4)
O4—V2—O2	94.1(3)	O26—B6—O25	106.9(9)	O15—V6—O8	106.0(4)
O11—V2—O3	107.2(3)	O26—B6—O5 <sup>i</sup>	110.0(8)	O2—V6—O8	92.4(3)
O4—V2—O3	145.9(3)	O25—B6—O5 <sup>i</sup>	109.5(8)	O15—V6—O1	111.0(4)
O2—V2—O3	78.8(3)	O26—B6—O18	112.6(9)	O2—V6—O1	78.7(3)
O11—V2—O5	108.9(4)	O25—B6—O18	111.3(8)	O8—V6—O1	142.8(3)
O4—V2—O5	78.1(3)	O5 <sup>i</sup> —B6—O18	106.4(8)	O15—V6—O9	108.2(4)
O2—V2—O5	144.1(3)	O26—B7—O9	112.1(9)	O2—V6—O9	142.3(3)
O3—V2—O5	88.3(3)	O26—B7—O27	106.4(9)	O8—V6—O9	77.7(3)
O12—V3—O5	110.5(4)	O9—B7—O27	108.8(9)	O1—V6—O9	87.5(3)
O12—V3—O6	109.0(4)	O26—B7—O17 <sup>i</sup>	113.4(9)	O20—B1—O19	122.2(10)
O5—V3—O6	138.3(3)	O9—B7—O17 <sup>i</sup>	108.8(9)	O20—B1—O21	117.0(10)
O12—V3—O4	107.2(4)	O27—B7—O17 <sup>i</sup>	107.1(8)	O19—B1—O21	120.7(10)
O5—V3—O4	77.9(3)	O28—B8—O29	118.1(10)	O22 <sup>i</sup> —B2—O7 <sup>i</sup>	110.4(8)

Continued Table 4

O6—V3—O4	78.3(3)	O28—B8—O27	120.3(10)	O22 <sup>i</sup> —B2—O19	106.2(8)
O12—V3—O17	107.0(4)	O29—B8—O27	121.5(10)	O7 <sup>i</sup> —B2—O19	108.4(8)
O5—V3—O17	90.4(3)	O1—B9—O30	110.7(9)	O22 <sup>i</sup> —B2—O16	112.7(8)
O6—V3—O17	90.5(3)	O1—B9—O29	112.3(9)	O7 <sup>i</sup> —B2—O16	109.5(8)
O4—V3—O17	145.8(3)	O30—B9—O29	106.7(9)	O19—B2—O16	109.6(8)
O13—V4—O8	108.0(4)	O1—B9—O17 <sup>i</sup>	108.2(9)	O6—B3—O30 <sup>i</sup>	110.4(9)
O13—V4—O4	108.4(4)	O30—B9—O17 <sup>i</sup>	110.6(9)	O6—B3—O20 <sup>i</sup>	108.9(9)
O8—V4—O4	93.9(3)	O29—B9—O17 <sup>i</sup>	108.2(8)	O30 <sup>i</sup> —B3—O20 <sup>i</sup>	105.6(9)
O13—V4—O7	106.9(4)	O8—V4—O6	144.9(3)	O6—B3—O16 <sup>i</sup>	110.6(9)
O8—V4—O7	78.6(3)	O4—V4—O6	78.0(3)	O30 <sup>i</sup> —B3—O16 <sup>i</sup>	111.4(9)

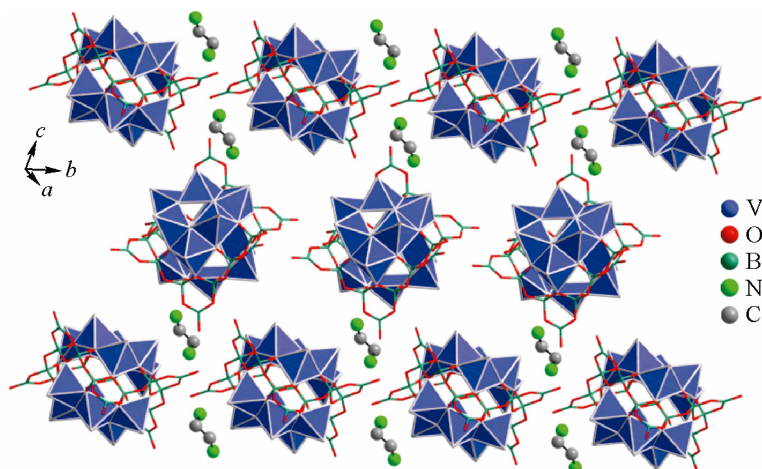
Symmetry codes: <sup>i</sup>  $-x-1, -y+1, -z$ .

Table 5

Hydrogen-bond geometry for **2**

D—H···A	D—H	H···A	D···A	D—H···A
N1—H1C···O49 <sup>v</sup>	0.89	2.04	2.823(13)	146
N1—H1D···O43 <sup>vi</sup>	0.89	2.37	2.934(13)	122
N1—H1D···O21 <sup>vii</sup>	0.89	2.15	2.930(14)	145
N1—H1E···O49 <sup>vi</sup>	0.89	2.40	2.830(14)	110
N2—H2C···O12 <sup>iv</sup>	0.89	2.16	2.930(2)	143
N2—H2D···O43 <sup>vi</sup>	0.89	2.09	2.910(2)	152
N2—H2D···O20 <sup>viii</sup>	0.89	2.43	2.850(2)	110
N2—H2D···O69W <sup>viii</sup>	0.89	2.35	2.980(2)	128
N2—H2E···O13 <sup>iv</sup>	0.89	2.16	3.010(2)	158
N2—H2E···O20 <sup>viii</sup>	0.89	2.57	2.850(2)	100

Symmetry codes: <sup>iv</sup>  $1+x, y, z$ ; <sup>v</sup>  $-1-x, -y, 1-z$ ; <sup>vi</sup>  $1+x, 1+y, z$ ;  
<sup>vii</sup>  $-x, 1-y, -z$ ; <sup>viii</sup>  $1-x, 1-y, 1-z$ .

Fig. 7. View of the crystalline packing of **2** in the plane (1 0 1)

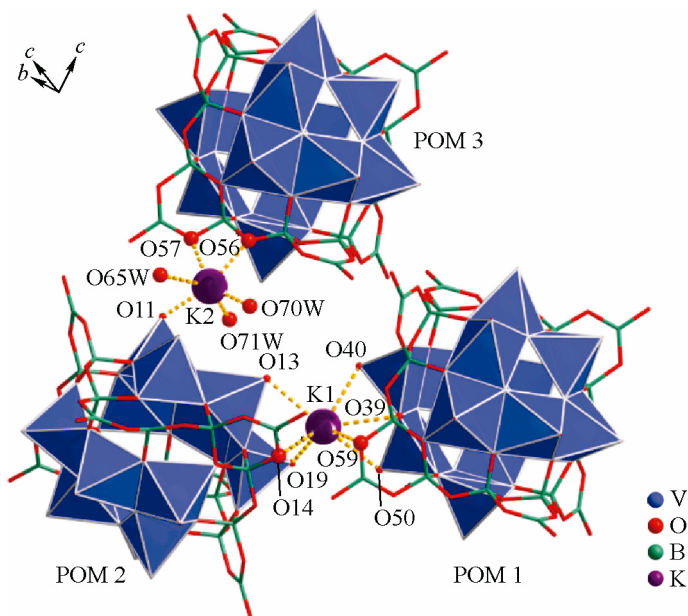


Fig. 8. Coordination sphere of K1 and K2 for 2

units, POM2 and POM3. The interaction to POM2 is K2—O11 (O vanadyl), 2.195 Å. The interactions to POM3 are K2—O56 ( $B_{\text{tet}}$ —O56— $B_{\text{tet}}$ ), 2.328 Å; K2—O57 ( $B_{\text{trig}}$ —O57— $B_{\text{tet}}$ ), 2.156 Å; the octahedral environment is completed by three water molecules, being the interactions K2—O65w, K2—O70w and K2—O71w with distances of 2.670 Å, 2.139 Å and 2.201, respectively.

**Structural comparison.** The crystallographic data, together with the BVS method [29], permits to assign a mixed valence ratio for the  $[\text{V}_{12}\text{B}_{18}\text{O}_{60}\text{H}_6]$  anionic cluster [30]. Using this methodology it is possible to infer that compounds (1) and (2) present an 11/1 ( $\text{V}^{\text{IV}}/\text{V}^{\text{V}}$ ) ratio.

Several compounds based on the  $[\text{V}_{12}\text{B}_{18}\text{O}_{60}\text{H}_6]^{n-}$  cluster with protonated ethylenediamine as compensating counterion have been previously reported [10–19], while only one lattice presenting protonated 1,3-diaminopropane (1,3-diapH<sub>2</sub>) as countercation is known, (1,3-diapH<sub>2</sub>)<sub>5</sub> $[\text{V}_{12}\text{B}_{18}\text{O}_{60}\text{H}_6] \cdot 6\text{H}_2\text{O}$  [17] (CCDC code REGHEQ). This reported crystalline lattice together with (1) present the 1,3-diapH<sub>2</sub> in the "W" conformation [31]. It is interesting to point out that the reported lattice presents the 1,3diapH<sub>2</sub> cations aligned in three different directions, while (1) presents the same cations aligned in only one direction in the lattice. This can be related to the fact that the reported structure by Rijssenbeek et al. is counterbalanced only by 1,3-diapH<sub>2</sub> cations, while (1) is also counterbalanced by hydronium and potassium cations. Moreover, (2) presents the protonated ethylenediamine cations also aligned in one direction. The reported structures by Lin et al. [18] and Lu et al. [19] which contain protonated ethylenediamine cations together with auxiliary cations such as sodium, potassium and hydronium also present this feature in the crystalline packing.

The presence of these auxiliary cations may be responsible for the alignment of the diamines in only one direction, since they can fill hindered nucleophilic sites around the polyanions.

The importance of the nature of the diprotonated diamine becomes evident, when the crystalline lattices of (1) and (2) are compared. Both compounds were obtained by similar synthetic conditions in the presence of MnCl<sub>2</sub>. However, in the preparation of (1) 1,3-diaminopropane was used, while in that of (2) this diamine was replaced by ethylenediamine. The resulting crystalline lattice for (1) presents the diprotonated diamine (1,3-diapH<sub>2</sub>) only in the bifurcated mode, while for (2) the diprotonated diamine (enH<sub>2</sub>) is not only in the bifurcated, but also in the trifurcated mode, i.e. a crystalline packing with more hydrogen bond interactions.

In this way it is possible to infer that the nature of the amine is a determining factor in the type of generated bonds in the respective lattices of the studied polyoxovanadoborate,  $[\text{V}_{12}\text{B}_{18}\text{O}_{60}\text{H}_6]$ .

Authors acknowledge FONDECYT 1120004 and Financiamiento Basal Program FB0807 for partial financial support. This work was done under the LIA-MIF CNRS 836 Collaborative Program. PHI thanks MECESUP UCH 0601 Doctoral Scholarship. PHI also thanks CONICYT AT-24100222 and TT-23120099 Doctoral Scholarships. Thanks are given to the Consejo Superior de Investigaciones Científicas (CSIC) of Spain for the award of a license for the use of the Cambridge Crystallographic Data Base (CSD).

#### REFERENCES

1. Streb C., Long D.-L., Cronin L. // CrystEngComm. – 2006. – **8**. – P. 629 – 634.
2. Yi Z., Yu X., Xia W., Zhao L., Yang C., Chen Q., Wang X.L., Xu X., Zhang X. // CrystEngComm. – 2010. – **12**. – P. 242 – 249.
3. Long D.-L., Kögerler P., Farrugia L.J., Cronin L. // Angew. Chem. Int. Ed. – 2003. – **42**. – P. 4180 – 4183.
4. Abbas H., Pickering A.L., Long D.-L., Kögerler P., Cronin L. // Chem. Eur. J. – 2005. – **11**. – P. 1071 – 1078.
5. Streb C., McGlone T., Brücher O., Long D.-L., Cronin L. // Chem. Eur. J. – 2008. – **14**. – P. 8861 – 8868.
6. McGlone T., Streb C., Long D.-L., Cronin L. // Chem. Asian. J. – 2009. – **4**. – P. 1612 – 1618.
7. Yan B., Xu Y., Bu X., Goh N.K., Chia L.S., Stucky G. // J. Chem. Soc. // Dalton Trans. – 2001. – P. 2009 – 2014.
8. Lisnard L., Dolbecq A., Mialane P., Marrot J., Sécheresse F. // Inorg. Chim. Acta. – 2004. – **357**. – P. 845 – 852.
9. Williams D., Wu M., Song H.H.-Y., Law T.S.-C., Zhang X.X. (Eds), Contemporary Boron Chemistry: Synthesis, Properties of Vanadoborate Cluster Materials, The Royal Society of Chemistry. – 2000. – P. 104 – 111.
10. Williams D., Wu M., Sung H.H.-Y., Zhang X.X., Yu J. // Chem. Commun. – 1998. – P. 2463 – 2464.
11. Cao Y.-N., Zhang H.-H., Huang C.-C., Sun Y.-X., Chen Y.-P., Guo W.-J., Zhang F.-L. // Chinese J. Struct. Chem. – 2005. – **24**. – P. 525 – 530.
12. Cai Q., Lu B., Zhang J., Shan Y. // J. Chem. Crystallogr. – 2008. – **38**. – P. 321 – 325.
13. Cao Y., Zhang H., Huang C., Yang Q., Chen Y., Sun R., Zhang F., Guo W. // J. Solid State Chem. – 2005. – **178**. – P. 3563 – 3570.
14. Warren C.J., Haushalter R.C., Rose D.J., Zubieta J. // Inorg. Chim. Acta. – 1998. – **282**. – P. 123 – 129.
15. Cao Y., Zhang H., Huang C., Chen Y., Sun R., Guo W. // J. Mol. Struct. – 2005. – **733**. – P. 211 – 216.
16. Sun Y.-Q., Li G.-M., Chen Y.-P. // Dalton Trans. – 2012. – **41**. – P. 5774 – 5777.
17. Rijssenbeek J.T., Rose D.J., Haushalter R.C., Zubieta J. // Angew. Chem. Int. Ed. Engl. – 1997. – **36**. – P. 1008 – 1010.
18. Lin Z.-H., Yang Q.-Y., Zhang H.-H., Huang C.-C., Sun R.-Q., Wu X.-Y. // Chinese J. Struct. Chem. – 2004. – **23**. – P. 590 – 595.
19. Lu B., Wang H., Zhang L., Dai C.-Y., Cai Q.-H., Shan Y.-K. // Chin. J. Chem. – 2005. – **23**. – P. 137 – 143.
20. SAINTPLUS Version 6.02; Bruker AXS: Madison, WI, 1999.
21. SHELXTL Version 5.1, Bruker AXS: Madison, WI, 1998.
22. Sheldrick G.M. // Acta Crystallogr. – 2008. – **A64**. – P. 112 – 122.
23. Sheldrick G.M. SHELXL-97, Program for Crystal Structure Refinement; University of Göttingen, Germany, 1997.
24. Brandenburg K. DIAMOND, Version 3.2i, Crystal Impact GbR, Bonn, Germany, 2012.
25. Desiraju G.R., Steiner T. The Weak Hydrogen Bond: In Structural Chemistry, Biology, Oxford University, 2001.
26. Steed J.W. // Coord. Chem. Rev. – 2001. – **215**. – P. 171 – 221.
27. Xiao X., Tao Z., Xue S.-F., Zhang Y.-Q., Zhu Q.-J., Liu J.-X., Wei G. // CrystEngComm. – 2011. – **13**. – P. 3794 – 3800.
28. Chen W.-J., Yu D.-H., Xiao X., Zhang Y.-Q., Zhu Q.-J., Xue S.-F., Tao Z., Wei G. // Inorg. Chem. – 2011. – **50**. – P. 6956 – 6964.
29. Brown D., Altermatt D. // Acta Cryst. – 1985. – **B41**. – P. 244 – 247.
30. Hermosilla-Ibáñez P., Car P.E., Vega A., Costamagna J., Caruso F., Pivan J.-Y., Le Fur E., Spodine E., Venegas-Yazigi D. // CrystEngComm. – 2012. – **14**. – P. 5604 – 5612.
31. Zhang Y.-N., Zhou B.-B., Sha J.-Q., Su Z.-H., Cui J.-W. // J. Solid State Chem. – 2011. – **184**. – P. 419 – 426.